CO gas sensing behavior of synthesized α-Fe₂O₃ nanorods fabricated via Alternative Current (AC) electric fields

Javad. Esmaeilzadeh[1], *Ebrahim. Zohourvahid Karimi[2]

[1]*Department of Nanotechnology and Advanced Materials, Materials and Energy Research Center, Tehran, Iran, 14155-4777*
[2]*Department of metallurgy and ceramic, Islamic Azad University, Mashhad Branch, Mashhad, Iran*
*Corresponding author's email address: ebrahimzk888@gmail.com

Abstract

In this work, the α-Fe₂O₃ nanorods with 50-100 nm in width were first synthesized by hydrothermal method. Thereafter, α-Fe₂O₃ nanorods were deposited within the gap of interdigitated platinum electrodes designed on an alumina sheet using print screen by employing the AC electrophoretic deposition technique at the frequency of 10 kHz. Finally, the gas sensing properties of the α-Fe₂O₃ nanorods toward CO gas (100-1600ppm) at 300-400 ℃were investigated. The results demonstrated that this sensor has suitable and rapid response as well as reasonable recovery times. The optimum temperature giving the highest response was achieved at 350℃. The response and recovery time for 900 ppm CO gas at optimal temperature was calculated to be 20 and 30 Sec, respectively.

Keywords: Fe₂O₃ nanorods, hydrothermal process, AC electrophoresis deposition, gas sensing properties

1. Introduction

Semiconductor gas sensors (metal oxide gas sensors) are electrical conductivity sensors. The resistance of their active sensing layer changes due to contact with the gas to be detected. Chemical gas sensors based on metal oxide semiconductors have received considerable attention for the detection of toxic and air contaminant gases such as CO owing to their chemical composition and properties [1-3]. CO is produced from incomplete combustion and is very toxic. Considering their distinctive electronic structure, different metal oxide semiconductors such as ZnO, In₂O₃, SnO₂, TiO₂ and Fe₂O₃ have been widely investigated for their gas sensing properties [4-6]. Among them, Hematite (α-Fe₂O₃) is an n-type semiconductor with band gap of 2.2eV and because of its nontoxicity, high stability under ambient conditions, low cost, and multi-functionality, is a good choice for a variety of application including catalysis [7], water splitting [8], and gas sensors [9,10].

The increasing demand for repeatable and fast detection of gases, the current researches in gas sensing techniques are focused on the development of gas sensors with good selectivity, rapid response, high sensitivity, and low cost. The origin of the sensing mechanism is attributed to the change of electrical resistance of the sensing material when it is exposed to a certain target gas at a given temperature [11]. Hence, the sensing performances are strongly dependent on the morphology, grain size, surface area, and dimensions. One-dimensional (1D) nanostructures are particularly suited for this application due to their high surface-to-volume ratio as well as good chemical and thermal stabilities under different operating conditions [12]. So far, various strategies such as electrospinning, template method and hydrothermal methods for producing of 1D nanostructures have been employed among which hydrothermal has the advantage of simple process, high yield and low cost[13, 14].

In addition to the sensing material itself, gas sensor performance is strongly affected by the morphology and structure of the sensing layer [15]. Thus; many efforts have been devoted to the improvement of the fabrication methods, since they determine these characteristics. Therefore, various deposition methods have been utilized such as melting and quenching, micro dropping, dip coating, screen printing, and sputtering for thick- or thin-film deposition. However, the complexities associated with each method make scientists look for new strategies to construct the sensing phase to attain the highest efficiency. AC electrophoretic deposition (ACEPD) [6, 16] is a method with high potentiality to deposit nanomaterials in a controlled manner. It is also a simple and reproducible way of the manipulation of ceramic nanostructures, their trajectory and alignment. In this study, we used ACEPD to deposit synthesized Fe_2O_3 nanorods onto interdigitated electrodes. The fabricated devices are exposed to various concentrations of CO for which the obtained results are presented.

2. Materials and Methods

2.1. Synthesis of α-Fe_2O_3 nanorods

All chemicals were analytical grade reagents used as-received without further purification. In the work reported here, 0.03 mol $FeCl_3.6H_2O$ (Sigma- Aldrich), and 1.2g poly-vinyl pyrrolidone (PVP, Sigma-Aldrich, $M_W=30000$) were added to 60 ml of deionized water. Then, the mixed solution was stirred under powerful magnetic stirring until a homogeneous solution was obtained. At the next step, the prepared solution was placed into a Teflon-lined stainless steel autoclave, sealed firmly, and heated at 120℃ for 12h. Thereafter, it was quenched down to room temperature. Reddish powder was separated by centrifugation, washed several times in deionized water and ethanol, and dried in air at 80℃. Finally, the precipitated products were calcined at 600℃ for 2h in air to obtain α-Fe_2O_3 nanorods. The powder morphology and crystal structure were characterized by SEM (Scanning Electron Microscopy, Cambridge-S360) and XRD (PHILIPS-PW3710, Bragg–Brentano geometry, Cu–K_α X-ray source, wavelength 1.5406Å, 20–85°), respectively. The size, morphology, and microstructure were observed by TEM (Transmission Electron Microscopy, TEM Philips CM200, and 200 kV)

2.2. Sensor fabrication and sensor response measurement

ACEPD was carried out in a deposition set-up consisting of a signal generator (Rigol, DG1022) and a voltage amplifier (HP, 6826A Signal Amplifier). 0.003 g of Fe_2O_3 nanorods were suspended in 10 ml pure acetone by ultrasonic and then deposited by ACEPD method on interdigitated electrodes in the frequency of 10 kHz, voltage of 25 V, and by a symmetric sinusoid wave. Deposition time was 10 min. The microstructure of the obtained deposit was analyzed using optical microscope (Olympus DP72) and SEM. The interdigitated platinum electrodes with a gap of 200 μm and designed on an alumina sheet were used for sensor fabrication. In order to reach the desired working temperature, this alumina-based sensor was equipped with a micro-heater on the backside of the sensor. The response of sensor toward various concentrations of CO gas (100-1600 ppm) at different temperatures was measured and recorded in a fully automated dynamic gas sensor testing setup, a schematic of which and the gas sensing circuit has been depicted in one of our previous works [5]. The sensor was stabilized before each sensing test by exposing to air for 1h. CO gas was diluted through mixing with air (base gas) using digital flow controller to reach pre-designed concentrations. Finally, the gaseous mixture was flown through a chamber equipped with the sensor.

3. Results and discussion

Fig. 1 shows the crystallographic information obtained from XRD analysis and SEM image of α-Fe_2O_3 nanorods calcined at 600 ℃. Fig.1a depicts the diffraction peaks that can be indexed to α-Fe_2O_3 (JCPDS No. 33-0664). No characteristics peaks were observed for other impurities and the XRD pattern is related to the pure rhombohedral structure of α-Fe_2O_3. Fig. 1b revealed the typical SEM image of products. As it can be seen, the α-Fe_2O_3 products were assembled by 1D nanostructures having bundle-like morphology.
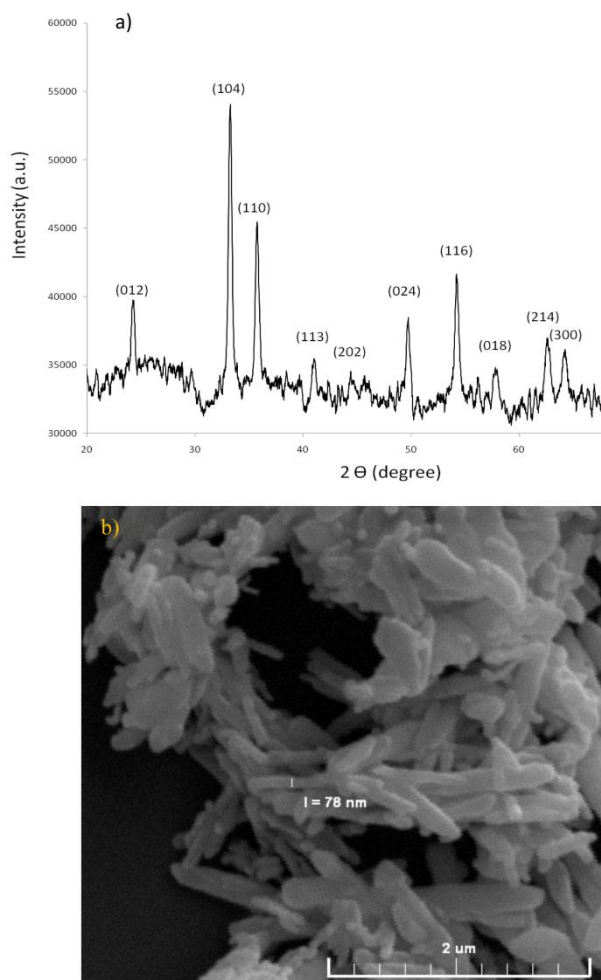
Fig. 1. X-ray diffraction pattern and SEM image of α- Fe_2O_3 nanorods

Further detailed information about the individual nanorods including size and morphology were obtained using TEM where the nanorods have smooth surface and a width of 50-100 nm (Fig.2). The optical image of the deposition pattern of α-Fe_2O_3 nanorods on interdigitated electrode is shown in Fig. 3. The deposition was carried out using AC electrophoretic deposition at frequency of 10 kHz where the sensing materials have filled the space between interdigitated electrodes with no materials left on electrode surface. In fact, the remained material on the surface of the electrode does not participate in the sensing process.
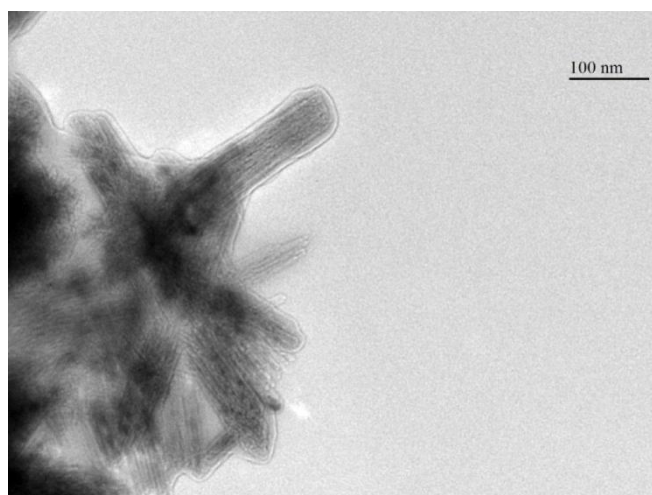
Fig. 2. Typical TEM images of α- Fe_2O_3 nanorods
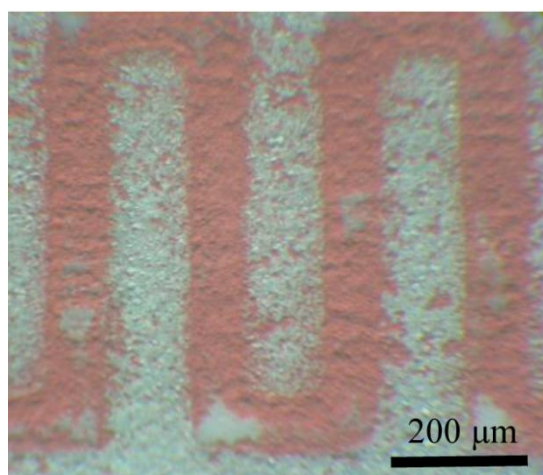
Fig. 3. Optical microscopy image of electrophoretically deposited α- Fe_2O_3 nanorods in the frequency of 10 kHz and voltage of 25 V on interdigitated platinum electrodes

The sensing layer which is deposited on the sensor base plate is shown in the SEM image of Fig. 4. It can be found that the nanorods are able to form chain-like structures into the space of electrodes at the deposition frequency of 10 kHz, which has been generally ascribed to the dielectrophoresis (DEP) force [17, 18]. This force has been exerted on polarized particles suspended in the colloidal suspension in the high-frequency AC electric field. The DEP force make nanorods move toward high intensity electric filed regions. When high frequency AC electric fields are applied to the nanorods/acetone system, suspended particles will be polarized and attracted by the DEP force toward the electrode edge where the electric field is strong. This filling of electrode space by α-Fe_2O_3 nanorods as sensing materials using AC EPD is a suitable structure for the fabrication of CO gas sensors. Also in Fig.4, it can be seen that the deposited sensing layers possess highly porous structures that is one of the features of the ACEPD technique. This porous deposited layer can provide high-diffusivity path for the target gas, maximizing the occurrence of surface reactions.
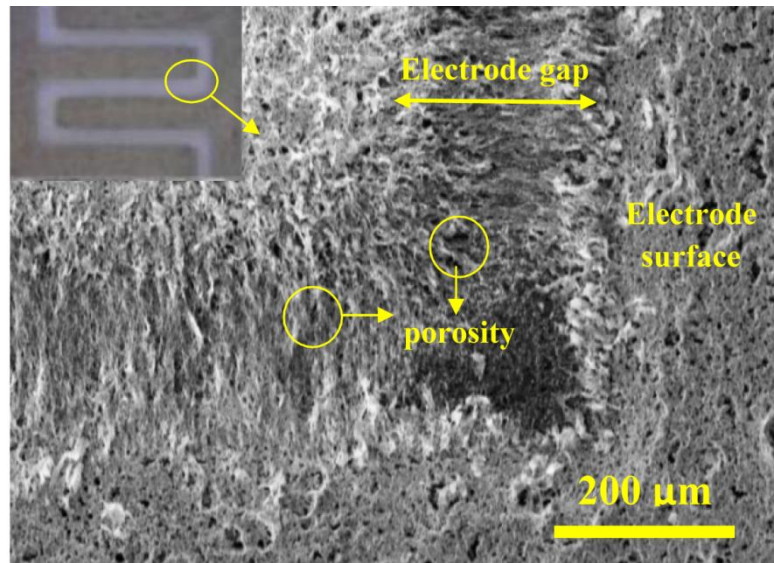
Fig. 4. SEM image of sensing layer deposited on the sensor base plate at the frequency of 10 kHz and voltage of 25 V

The values of gas sensor response based on α-Fe_2O_3 nanorods to different CO concentrations from 100 to 1600 ppm, operating in the temperature range of 300-400℃ are plotted in Fig. 5. The sensor response is calculated by $\frac{R_{air} - R_{gas}}{R_{gas}} \times 100$ where R_{air} and R_{gas} are the resistance of the sensor exposed to the base gas (air) and CO as target gas, respectively.
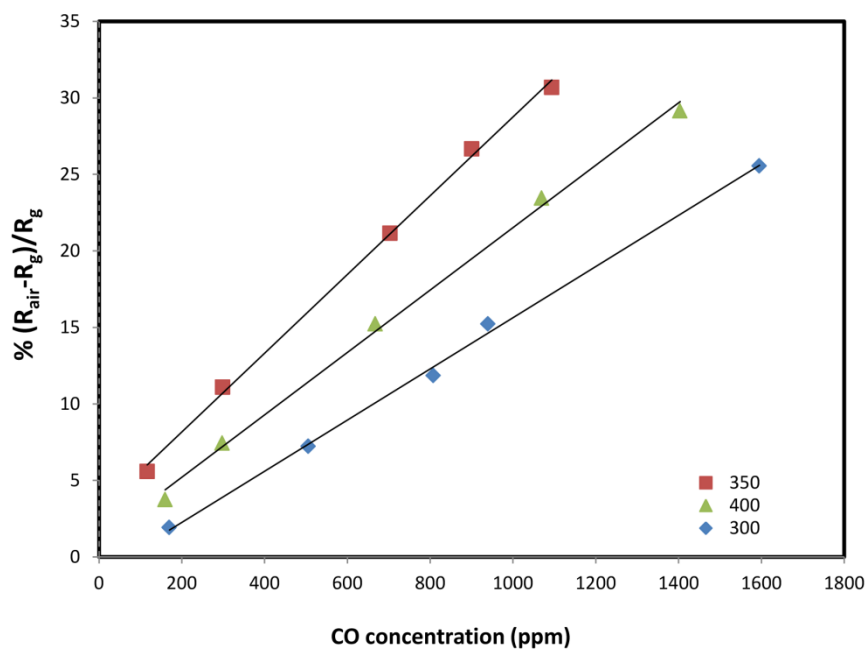
Fig. 5. Response values of sensor toward different CO concentrations at the temperature range of 300–400 ℃

As it is shown, at each operating temperature, the response of gas sensor possesses rising linear trend by increasing in gas concentration. It is well-known that the performance of semiconductor gas sensors is strongly affected by its operating temperature [9]. In order to find the optimum operating temperature the gas sensor was tested on different working temperature between 300℃ to 400℃. Since the conductance of these sensors became too low for practical temperature less than 300℃, the working temperature of sensor was chosen above 300℃. As it can be observed in Fig. 5, the sensor response increased by increasing the working temperature up to 350℃, while further increase in temperature decreased the sensor response. At elevated temperatures, the desorption rate of the target gas molecules on the surface of the sensing material is higher than the adsorption rate of the gas. So, the reversibility of the sensor is severely reduced and response value is decreased [6].

The optimum operating temperature giving the highest response has been determined as 350℃ for all tested sensors under different concentrations of CO gas. The response and recovery behavior of sensors were further evaluated by orderly exposure to different concentrations of CO gas at the temperature range of 300-400 ℃. Fig. 6a illustrates the cyclic response curve of this sensor showing the resistance change of sensor for different concentration of CO gas at 350–450 ℃. The sensor shows a relatively stable baseline resistance in each on-off cycle, especially at elevated temperature, guaranteeing long term application. The gas-sensing curves in Fig. 6a and 6b indicate the expected sensing mechanism of n-type semiconductors based on surface chemisorption of the reducing gas molecules and electron donation. When the Fe_2O_3 gas sensor is exposed to air (base gas), the oxygen molecules are adsorbed on Fe_2O_3 nanorods surface, leading to capturing of the conduction band electrons.

$$O_{2(g)} \longrightarrow 2O_{ads}^{-}$$

This adsorbed oxygen then reacts with CO gas according to the following reaction:

$$CO_g + O_{ads}^{-} \longrightarrow CO_{2(g)} + e^{-}$$

This will release the electrons back to the conduction band of Fe_2O_3 nanorods which induced a decrease in resistance [19].

The cyclic curve of sensors operating in the temperature of 350℃ giving the highest response with channel composed of 900 ppm of CO gas is shown in Fig. 6b. At first glance, in terms of sensor stability, no significant change was observed in the sensor response curve after several cycles which ensure the stability of the sensor. Besides, no overshooting is seen in the resistance variation. The other characteristic of the sensor is the fast responses while exposing to gas or shutting the gas off. The response and recovery times calculated from the cyclic curve of sensor for 900 ppm CO are as short as 20 sec and 30 sec, respectively. These values are calculated based on the time period during which the resistance of sensing layer reaches to 90% of the saturated resistance (when switching to the target gas) and 10% of the saturated resistance (after switching back to air as the base gas), respectively.
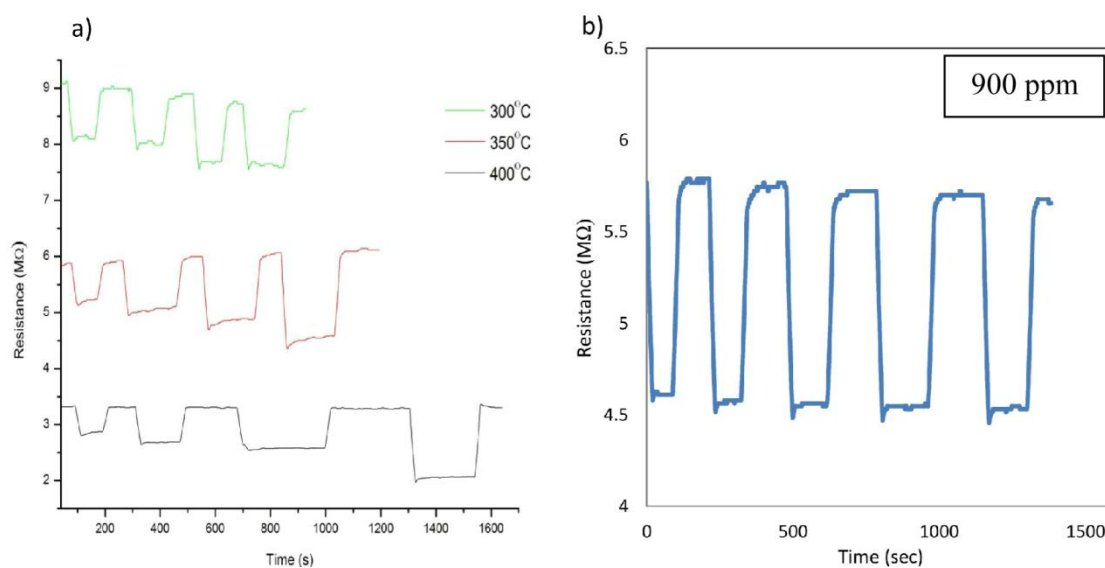
Fig. 6. (a) Dynamic response curves of gas sensor toward different CO concentration at the operating temperature range of 300–400 ℃, (b) Cyclic curve of sensor response to 900 ppm of CO gas at 350 ℃

As mentioned earlier, based on the gas sensing mechanism, the sensor performances are influenced by three levels of physisorption, chemisorption, and the final desorption. According to Sun *et al.* [14] and Karimi *et al.* [15], grain junctions of the bundle-like nanostructures as active sites and high surface to volume ratio of nanorods as sensing materials and also randomly aligning of nanorods inter space of sensing electrodes on ACEPD provide the maximum reactions of target gas with sensing materials, so this sensor has a rapid response and recovery times.

CONCLUSION

In summary, α-Fe_2O_3 nanorods were successfully synthesized through a simple hydrothermal method. Crystallography information of nanorods indicated that the synthesized nanostructures are purely rhombohedral. The ACEPD technique was applied to fabricate a gas sensor at frequency of 10 kHz. This technique is able to deposit nanorods within the electrode gap, leaving behind no materials on the electrode surface. The sensing properties of the fabricated sensor at working temperature of 300–400 ℃ toward 100–1600 ppm CO demonstrated that the highest response was obtained at 350℃, whereas response and recovery time sare about 20 and 30 sec, respectively. The results confirmed that the electrophoretic assembly has a great potential for fabricating sensors based on Fe_2O_3 nanorods with adequate properties.

REFERENCES

1. Gardeshzadeh A.R, Raissi B, Marzbanrad E, Mohebbi H.. Fabrication of resistive CO gas sensor based on SnO_2 nanopowders via low frequency AC electrophoretic deposition. J Mater Sci: Mater Electron 20, 2009, 127–131.
2. Esmaeilzadeh J, Marzbanrad E, Zamani C, Raissi B. Fabrication of undoped-TiO_2 nanostructure-based NO_2 high temperature gas sensor using low frequency AC electrophoretic deposition method, Sens Actuators B: Chem 161, 2012, 401–405

3. 3.A. Kolmakov, Y.X. Zhang, G.S. Cheng, M. Moskovits. Detection of CO and O_2 using tin oxide nanowire sensors, Adv. Mater. 15, 2003, 997–1000

4. Sowti khiabani P, Marzbanrad E, Zamani C, Riahifar R, Raissi B. Fabricationof In_2O_3 based NO_2 gas sensor through AC-electrophoretic deposition. Sens Actuators B: Chem 166–167, 2012, 128–134

5. Esmaeilzadeh J, Ghashghaie S, Raissi B, Marzbanrad E, Zamani C, Riahifar R. Dispersant-assisted low frequency electrophoretically deposited TiO_2 nanoparticles in non-aqueous suspensions for gas sensing applications. J Ceram Int 38, 2012, 5613–5620

6. Esmaeilzadeh J, Ghashghaie S, Sowti khiabani P, Hosseinmardi A, Marzbanrad E, Raissi B, Zamani C. Effect of dispersant on chain formation capability of TiO_2nanoparticlesunder low frequency electric fields for NO_2 gas sensing applications, J Eur Ceram Society 34, 2014, 1201–1208

7. 7.Xiaobo Wang , Keting Gui. Fe_2O_3 particles as superior catalysts for low temperature selective catalytic reduction of NO with NH_3, J Envi Sci, 2, 2013, 2469–2475

8. Gul Rahman, Oh-Shim Joo. Photo electrochemical water splitting at nanostructured α-Fe_2O_3 electrodes, Int J Hydrogen Energ, 37, 2012, 13989–13997

9. Yali Cao, Haiyang Luo, Dianzeng Jia. Low-heating solid-state synthesis and excellent gas-sensing properties of α-Fe_2O_3 nanoparticles, Sens Actuators B 176, 2013, 618– 624

10. X.H. Hu, J.C. Yu, J.M. Gong, Q. Li, G.S. Li. α-Fe_2O_3 nanorings prepared by a microwave-assisted hydrothermal process and their sensing properties", Adv.Mater., 19 , 2007, 2324–2329

11. N. Barsan, D. Koziej. U. Weimar, Metal oxide-based gas sensor research: how to? Sens. Actuators B: Chem. 121 , 2007, 18–35

12. Comini E, Baratto C, Faglia G, Ferroni M, Vomiero A, Sberveglieri G. Quasi-one dimensional metal oxide semiconductors: Preparation, characterization and application as chemical sensors, Prog. Mater Sci, 54 , 2009, 1-67

13. Mohammadi-kish M. Hydrothermal synthesis, characterization and optical properties of ellipsoid shape α-Fe_2O_3 nanocrystals, J Ceram Int 40, 2014, 1358-1361

14. Peng Sun, Lu You, Dawei Wang, Yanfeng Sun, Jian Ma, Geyu Lu. Synthesis and gas sensing properties of bundle-like α-Fe_2O_3 nanorods, Sens. Actuators B: Chem 156, . 2011, 368–374

15. E.Z.Karimi, J. Esmaeilzadeh, E. Marzbanrad. Electrospun TiO_2 nanofibers-based gas sensors fabricated by AC electrophoresis deposition, Bull. Mater. Sci. 38, 2015, 1-6

16. 16.R. Riahifar, B. Raissi, E. Marzbanrad, C. Zamani. Effect of parameters on deposition pattern of ceramic nanoparticles in non-uniform AC electric field, J. Mater. Sci. Mater. Electron, 22, 2011, 40-46

17. 17.Ronald Pethig. Review Article—Dielectrophoresis: Status of the theory, technology, and applications, Biomicrofluidics 4, 2010, 228- 241

18. Robert Kretschmer and Wolfgang Fritzsche. Pearl Chain Formation of Nanoparticles in Microelectrode Gaps by Dielectrophoresis, Langmuir 20, 2004, 11797-11801

19. J.S. Han , D.E. Davey , D.E. Mulcahy , A.B. Yu. Effect of the pH value of the precipitation solution on the CO sensitivity of α-Fe_2O_3, Sens. Actuators B: Chem 61, 1999, 83–91